Article:

Dowker, M. and Ohkitani, K. (2012) Intermittency and local Reynolds number in Navier-Stokes turbulence: A cross-over scale in the Caffarelli-Kohn-Nirenberg integral. Physics of Fluids, 24 (11). 115112. ISSN: 1070-6631

https://doi.org/10.1063/1.4767728

Intermittency and local Reynolds number in Navier-Stokes turbulence: a cross-over scale in the Caffarelli-Kohn-Nirenberg integral

Mark Dowker and Koji Ohkitani

School of Mathematics and Statistics,

University of Sheffield, Hicks Building,

Hounsfield Road, Sheffield S3 7RH, United Kingdom

(Dated: October 16, 2012)

Abstract

We study space-time integrals which appear in Caffarelli-Kohn-Nirenberg (CKN) theory for the Navier-Stokes equations analytically and numerically. The key quantity is written in standard notations $\delta(r) = 1/(\nu r) \int_{Q_r} |\nabla \boldsymbol{u}|^2 \, d\boldsymbol{x}\, dt$, which can be regarded as a local Reynolds number over a parabolic cylinder Q_r.

First, by re-examining the CKN integral we identify a cross-over scale $r_* \propto L \left(\frac{\overline{\|\nabla \boldsymbol{u}\|_{L^2}^2}}{\|\nabla \boldsymbol{u}\|_{L^\infty}^2} \right)^{1/3}$, at which the CKN Reynolds number $\delta(r)$ changes its scaling behavior. This reproduces a result on the minimum scale $r_{\rm min}$ in turbulence: $r_{\rm min}^2 \|\nabla \boldsymbol{u}\|_\infty \propto \nu$, consistent with a result of Henshaw *et al.* (1989). For the energy spectrum $E(k) \propto k^{-q}$ $(1 < q < 3)$, we show that $r_* \propto \nu^a$ with $a = \frac{4}{3(3-q)} - 1$. Parametric representations are then obtained as $\|\nabla \boldsymbol{u}\|_\infty \propto \nu^{-(1+3a)/2}$ and $r_{\rm min} \propto \nu^{3(a+1)/4}$. By the assumptions of the regularity and finite energy dissipation rate in the inviscid limit, we derive $\lim_{p\to\infty} \frac{\zeta_p}{p} = 1 - \zeta_2$ for any phenomenological models on intermittency, where ζ_p is the exponent of p-th order (longitudinal) velocity structure function. It follows that $\zeta_p \leq (1-\zeta_2)(p-3)+1$ for any $p \geq 3$ *without* invoking fractal energy cascade.

Second, we determine the scaling behavior of $\delta(r)$ in direct numerical simulations of the Navier-Stokes equations. In isotropic turbulence around $R_\lambda \approx 100$ starting from random initial conditions, we have found that $\delta(r) \propto r^4$ *throughout the inertial range*. This can be explained by the smallness of $a \approx 0.26$, with a result that r_* is in the energy-containing range. If the β-model is perfectly correct, the intermittency parameter a must be related to the dissipation correlation exponent μ as $\mu = \frac{4a}{1+a} \approx 0.8$ which is larger than the observed $\mu \approx 0.20$.

Furthermore, corresponding integrals are studied using the Burgers vortex and the Burgers equation. In those single-scale phenomena, the cross-over scale lies in the dissipative range. The scale r_* offers a practical method of quantifying intermittency. This paper also sorts out a number of existing mathematical bounds and phenomenological models on the basis of the CKN Reynolds number.

PACS numbers: Valid PACS appear here

I. INTRODUCTION

The question of regularity of the three-dimensional Navier-Stokes equations is one of the most prominent unsolved problems in mathematics. The relevance of this issue exceeds that of pure mathematics, as the equations themselves represent an important physical process of turbulence. The integrity of this model, and our interpretation of the related physics involved, thus rests on whether the equations do admit unique classical solutions.

It is well-known that in the two-dimensional case the regularity is maintained with unique smooth solutions being defined for all time. This is the case because the quantity $\|\boldsymbol{\omega}\|_{L^2}^2$ is bounded from above for all time. In the case of three dimensions, however, this is known to hold for short time intervals only, assuming sufficiently smooth initial conditions. This cannot be guaranteed for an arbitrary time interval due to the vortex-stretching term, which is absent in two dimensions. At high Reynolds numbers, where turbulence becomes pronounced, the possibility that the Navier-Stokes equations may develop finite time singularities cannot be ruled out [1–5].

There have been many previous attempts to tackle the regularity problem, notably Leray [6], who first introduced the concept of weak solutions, followed by Hopf [7]. Later Scheffer [8], subsequently refined by Caffarelli, Kohn and Nirenberg (hereafter, CKN) [9], set limits on the dimension of the possible singular set of solutions. Others have produced a range of global weak, and local or particular strong solutions, but the existence of global classical solutions has not yet been established for general smooth initial conditions.

This mathematical problem is connected with the problem of turbulence. A conventional picture of energy cascade in 3D Navier-Stokes turbulence goes as follows. For a flow with huge Reynolds number $Re = UL/\nu > Re_{\text{cr}}$, where U, L, ν and Re_{cr} denote the characteristic velocity, length scale, kinematic viscosity and critical Reynolds number, respectively. The large-scale disturbances are subject to instability and they generate disturbances with a length scale l_1 and velocity scale v_1. The corresponding Reynolds number $Re_1 = v_1 l_1/\nu$ is still large and first-order disturbances are unstable and break down, resulting in smaller length l_2 and velocity v_2, whose Reynolds number is $Re_2 = v_2 l_2/\nu$. This process continues until the n-th step whose Reynolds number $Re_n = v_n l_n/\nu$ becomes $O(1)$, or on the order of Re_{cr}. In a nutshell, the regularity can be monitored by watching a suitably defined local Reynolds number. The CKN criterion was originally developed for testing the regularity of Navier-Stokes flows, but here we will show how useful it is in the characterization of intermittency in turbulence. See also [10] for another approach to intermittency.

In recent years, much progress has been made, both analytically (see in particular [3], [11] and [12]) and numerically. There have been numerous contributions to the field from the latter perspective, of which mention here only a few closely related to the main focus of the present paper. In particular, studies of possible singularities [13–15] and the monitoring of enstrophy and vorticity growth rates [16, 17]. See also [18–31] for various aspects of the Navier-Stokes equations.

In Section II we introduce the equations that will be the main subject of study of the paper. Section III presents numerical results on the scaling of the CKN integral. Section IV gives examples by exact solutions. Section V is devoted to a summary and discussion.

II. MATHEMATICAL FORMULATION

A. Caffarelli-Kohn-Nirenberg integrals

The three-dimensional Navier-Stokes equations

$$\frac{\partial \boldsymbol{u}}{\partial t} + (\boldsymbol{u} \cdot \nabla)\boldsymbol{u} = -\nabla p + \nu \nabla^2 \boldsymbol{u} + \boldsymbol{F}, \tag{1}$$

together with the continuity equation

$$\nabla \cdot \boldsymbol{u} = 0, \tag{2}$$

describe the motion of viscous incompressible fluids, where $\boldsymbol{u}$ denotes the fluid velocity, p the pressure, ν the kinematic viscosity and $\boldsymbol{F}$ the external body force, with appropriate initial and boundary conditions.

These equations can be transformed into vorticity equations

$$\frac{\partial \boldsymbol{\omega}}{\partial t} + (\boldsymbol{u} \cdot \nabla)\boldsymbol{\omega} = (\boldsymbol{\omega} \cdot \nabla)\boldsymbol{u} + \nu \nabla^2 \boldsymbol{\omega} + \nabla \times \boldsymbol{F}, \tag{3}$$

where $\boldsymbol{\omega} = \nabla \times \boldsymbol{u}$ is the vorticity.

The function $\delta(r)$ is a local average of $\nabla \boldsymbol{u}$ over a parabolic cylinder. This non-dimensional quantity is defined by the space-time integral

$$\delta(r) = \frac{1}{\nu r} \int_{Q_r} |\nabla \boldsymbol{u}|^2 \, d\boldsymbol{x}\, dt, \tag{4}$$

where r is the distance from the center point $\boldsymbol{x}_0$. The integral is taken over the space-time region, a parabolic cylinder,

$$Q_r(\boldsymbol{x},t) = \left\{ (\boldsymbol{x},t) : |\boldsymbol{x}-\boldsymbol{x}_0| < r,\ t_0 < t < t_0 + \frac{r^2}{\nu} \right\}, \tag{5}$$

where $\boldsymbol{x} = (x,y,z)$, with a center point $\boldsymbol{x}_0 = (x_0,y_0,z_0)$ and reference time t_0. Here the four-dimensional space-time volume of the parabolic cylinder (5) is given by $|Q_r| = 4\pi r^3/3 \cdot r^2/\nu = 4\pi r^5/3\nu$. The function $\delta(r)$ depends on the center point $(\boldsymbol{x}_0,t_0)$, but this dependence is made implicit for simplicity of notations.

According to the CKN theory [9, 29, 30], if $\delta(r) \leq \epsilon_{CKN}$ near $(\boldsymbol{x}_0,t_0)$, where ϵ_{CKN} is a positive constant, then $(\boldsymbol{x}_0,t_0)$ is a regular point, that is, the velocity must be bounded there. In fact, the CKN theory refines Scheffer's previous estimate [8], to show that the Hausdorff dimension of the possible singular sets of velocity in $(3+1)$-dimensional space-time does not exceed 1. See [32, 33] for more recent works.

We may interpret $\delta(r)$ as the local Reynolds number as follows [30]

$$Re = \frac{r^2}{\nu}\left(\frac{1}{|Q_r|}\int_{Q_r} |\nabla \boldsymbol{u}|^2 \, d\boldsymbol{x}\, dt\right)^{1/2} = \left(\frac{3}{4\pi}\delta(r)\right)^{1/2}. \tag{6}$$

We will study the following questions: What kind of scaling behavior do we expect for $\delta(r)$? and in which range are these power-laws observed ?

We consider a theory for the case of $\mathbb{R}^3$ first and then translate the result to the case of $\mathbb{T}^3$ or homogeneous turbulence. Let us consider the total kinetic energy, the enstrophy and the energy dissipation rate

$$E' = \int_{\mathbb{R}^3} \frac{|\boldsymbol{u}|^2}{2} d\boldsymbol{x},\ Q' = \int_{\mathbb{R}^3} \frac{|\nabla \boldsymbol{u}|^2}{2} d\boldsymbol{x},\ \epsilon' = \nu \int_{\mathbb{R}^3} |\nabla \boldsymbol{u}|^2 d\boldsymbol{x},$$

where $'$ denotes total spatial integrals in $\mathbb{R}^3$.

We examine the power-laws for $\delta(r)$ by examining the definition (4). A normalization of (4) over the volume gives

$$\delta(r) = \frac{4\pi}{3}\frac{r^4}{\nu^2}\frac{1}{|Q_r|}\int_{Q_r} |\nabla \boldsymbol{u}|^2 \, d\boldsymbol{x}\, dt,$$

which means that in the limit of $r \to 0$ we have

$$\delta(r) \to \frac{4\pi}{3}\frac{r^4}{\nu^2} |\nabla \boldsymbol{u}|^2 (\boldsymbol{x}_0,t_0), \tag{7}$$

picking up a point-wise value of the strain rate at $(\boldsymbol{x}_0, t_0)$. On the other hand, in the limit of $r \to \infty$ we have

$$\delta(r) \to \frac{r}{\nu^2}\frac{1}{r^2/\nu}\int_{t_0}^{t_0+r^2/\nu} dt \int_{\mathbb{R}^3} |\nabla \boldsymbol{u}|^2 \, d\boldsymbol{x} = \frac{r}{\nu^2}\overline{\int_{\mathbb{R}^3} |\nabla \boldsymbol{u}|^2 \, d\boldsymbol{x}}, \tag{8}$$

where the bar denotes a long time-average. Hence, the function $\delta(r)$ shows two distinctive behaviors and the cross-over takes place at $r = r_*$, where

$$r_* = \left(\frac{3}{4\pi} \frac{\overline{\int_{\mathbb{R}^3} |\nabla \boldsymbol{u}|^2 \, d\boldsymbol{x}}}{\|\nabla \boldsymbol{u}\|_\infty^2} \right)^{1/3} = \left(\frac{3}{4\pi} \frac{\overline{\epsilon'}}{\nu \|\nabla \boldsymbol{u}\|_\infty^2} \right)^{1/3}. \tag{9}$$

Because small-scale structure of finite-energy turbulence is expected to be not much different from that of homogeneous turbulence [34], the above expression translates to

$$r_* = L \left(\frac{3}{4\pi} \frac{\frac{1}{L^3}\overline{\int_{\mathbb{T}^3} |\nabla \boldsymbol{u}|^2 \, d\boldsymbol{x}}}{\|\nabla \boldsymbol{u}\|_\infty^2} \right)^{1/3} = L \left(\frac{3}{4\pi} \frac{\overline{\epsilon}}{\nu \|\nabla \boldsymbol{u}\|_\infty^2} \right)^{1/3} \tag{10}$$

in the case of $\mathbb{T}^3$. Here $\epsilon = \frac{\nu}{L^3} \int_{\mathbb{T}^3} |\nabla \boldsymbol{u}|^2 \, d\boldsymbol{x}$ is the energy dissipation rate per unit volume. Solving (10) for $\|\nabla \boldsymbol{u}\|_\infty$, we find

$$\|\nabla \boldsymbol{u}\|_\infty \approx \sqrt{\frac{3}{4\pi}} \sqrt{\frac{\overline{\epsilon}}{\nu}} \left(\frac{L}{r_*} \right)^{3/2}. \tag{11}$$

Plugging this into (7) and assuming that the maximum strain is attained at $\boldsymbol{x}_0$, we find

$$\delta(r) \approx \left(\frac{L}{r_*} \right)^3 \frac{\overline{\epsilon} r^4}{\nu^3} \tag{12}$$

for small r. By demanding that $\delta(r_{\min}) = 1$ because the cascade terminates when the local Reynolds number becomes $O(1)$, we determine the smallest scale excited in the flow as

$$r_{\min} \approx \left(\frac{\nu^3}{\overline{\epsilon}} \right)^{1/4} \left(\frac{r_*}{L} \right)^{3/4}. \tag{13}$$

Eliminating r_* from (11) and (13), we obtain a condition

$$r_{\min}^2 \|\nabla \boldsymbol{u}\|_\infty \propto \nu.$$

This is equivalent to a rigorous result on the estimate of the smallest length scale in turbulence [35, 36]

$$r_{\min} \propto \sqrt{\frac{\nu}{\|\nabla \boldsymbol{u}\|_\infty}}.$$

We note that this estimate can also be obtained by the methods of ladder inequalities [2]. It is defined as a reciprocal of the wavenumber therein, beyond which Fourier coefficients decay exponentially. See also [37] on how the minimum scale is affected by intermittency. In what follows, we will write simply ϵ for $\overline{\epsilon(t)}$ because its temporal fluctuations are not large.

B. The ν-dependence of r_*

We show that a power-law of r_* follows from that of $E(k)$. The following assumptions are made in the subsequent argument.

1. The energy dissipation rate ϵ and viscosity ν are independent in the inviscid limit.

2. The energy spectrum follows $E(k) \propto k^{-q}$ in the inertial subrange, with $1 < q < 3$.

3. An ensemble and a spatial averages are equal (ergodic hypothesis).

4. The velocity gradient is finite for a small, but fixed ν.

We write

$$\frac{r_*}{L} = F(\nu),$$

because if F were independent of ν, we would have non-intermittent turbulence (K41). We have therefore

$$\|\nabla \boldsymbol{u}\|_\infty \propto \sqrt{\frac{\epsilon}{\nu}} F(\nu)^{-3/2} \tag{14}$$

and

$$r_{\mathrm{min}} \approx \left(\frac{\nu^3}{\epsilon}\right)^{1/4} F(\nu)^{3/4}. \tag{15}$$

By the assumptions 1), 2) and the definition of ϵ

$$\epsilon = 2\nu \int_0^{k_d} k^2 E(k) dk$$

together with $k_d = 1/r_{\mathrm{min}}$, we have

$$\epsilon \approx \frac{2\nu}{3-q} \left(\left(\frac{\nu^3}{\epsilon}\right)^{-\frac{1}{4}} F(\nu)^{-\frac{3}{4}} \right)^{3-q}.$$

It follows that

$$F(\nu) \approx \left(\frac{2}{3-q} \frac{\nu}{\epsilon}\right)^{\frac{4}{3(3-q)}} \left(\frac{\nu^3}{\epsilon}\right)^{-\frac{1}{3}},$$

that is,

$$F(\nu) \propto \nu^a,$$

where

$$a \equiv \frac{4}{3(3-q)} - 1. \tag{16}$$

Thus, r_* also has a power-law dependence on ν. Inverting (16) we obtain

$$q = \frac{5+9a}{3(1+a)}. \tag{17}$$

C. Parametrization of intermittency via a

By writing

$$\frac{r_*}{L} = \left(\frac{\eta}{L}\right)^{4a/3} \propto \nu^a,$$

we find from (11) and (13)

$$\|\nabla \boldsymbol{u}\|_\infty \approx \sqrt{\frac{3}{4\pi}}\sqrt{\frac{\epsilon}{\nu}}\left(\frac{L}{\eta}\right)^{2a}, \tag{18}$$

and

$$r_{\min} \approx \eta \left(\frac{\eta}{L}\right)^a \tag{19}$$

as parameterizations of the maximum strain and the minimum scale excited in turbulence. We also note in passing that Kolmogorov velocity (with intermittency effect taken into account) is given by

$$v_{\mathrm{Kol}} \propto (\epsilon\nu)^{1/4}\left(\frac{L}{\eta}\right)^a$$

and acceleration A by

$$A \propto \frac{v_{\mathrm{Kol}}^3}{\nu}.$$

To summarize, in terms of a we have the following parameterizations

$$\|\nabla \boldsymbol{u}\|_\infty \propto \nu^{-\frac{1+3a}{2}},\ r_{\min} \propto \nu^{\frac{3(a+1)}{4}},\ r_* \propto \nu^a. \tag{20}$$

On the other hand, under the assumption of the β-model [38], we can write

$$\|\nabla \boldsymbol{u}\|_\infty \propto \nu^{-\frac{5-D}{1+D}},\ r_{\min} \propto \nu^{\frac{3}{1+D}},\ r_* \propto \nu^{\frac{3-D}{1+D}} \tag{21}$$

in terms of the self-similarity dimension D. Equivalently, under the same assumption, using the exponent of dissipation correlation $\mu = 3 - D$, we have

$$\|\nabla \boldsymbol{u}\|_\infty \propto \nu^{-\frac{2+\mu}{4-\mu}},\ r_{\min} \propto \nu^{\frac{3}{4-\mu}},\ r_* \propto \nu^{\frac{\mu}{4-\mu}}. \tag{22}$$

Note that the parametrization in terms of a does not require the assumption of fractal cascade. In Table I we compare some phenomenological models of intermittency [34, 38, 39]. The extreme case of intermittency $E(k) \propto k^{-8/3}$, beyond which no energy cascade can be sustained, was obtained using the Euler equations in [34] and with weak solutions of the Navier-Stokes equations in [40].

TABLE I: Comparison of models of intermittency

	General	K41	Ruelle	She-Leveque (SL)	Burgers	Sulem-Frisch (SF)
Intermittency exponent	a	0	1/9	1/5	1/3	3
D	$\frac{3-a}{1+a}$	3	13/5	7/3	2	0
μ	$\frac{4a}{1+a}$	0	2/5	2/3	1	3
$\\|\nabla \boldsymbol{u}\\|_\infty$	$\nu^{-(1+3a)/2}$	$(\epsilon/\nu)^{1/2}$	$\nu^{-2/3}$	$\nu^{-4/5}$	ν^{-1}	ν^{-5}
$r_{\min}$	$\nu^{3(a+1)/4}$	$\eta = \left(\nu^3/\epsilon\right)^{1/4}$	$\nu^{5/6}$	$\nu^{9/10}$	ν	ν^3
v_{Kol}	$\nu^{(1-3a)/4}$	$(\epsilon\nu)^{1/4}$	$\nu^{1/6}$	$\nu^{1/10}$	ν^0	ν^{-2}
Hölder continuity	$C^{\frac{1-3a}{3(1+a)}}$	$C^{1/3}$	$C^{1/5}$	$C^{1/9}$	C^0	$C^{-2/3}$
$E(k) \propto k^{-q}$	$q = \frac{5+9a}{3(1+a)}$	$q = 5/3$	$q = 9/5$	$q \approx 5/3 + 0.03 < 17/9$	$q = 2$	$q = 8/3$

In [39], the distribution of Lyapunov exponents for the Navier-Stokes equations was studied and its behavior was found to change at $\mu = 2/5$ on the basis of the β-model. In [41], a model of intermittency was developed on the basis of log-Poisson statistics of the energy dissipation rate, which shows agreement with experiments. We note that in [42] a scaling $r_{min} \propto \nu$ was suggested for low-Reynolds number turbulence, which corresponds to $a = 1/3$. See also references cited therein. The relationship $a = \mu/(4-\mu)$ is depicted in Fig.1.

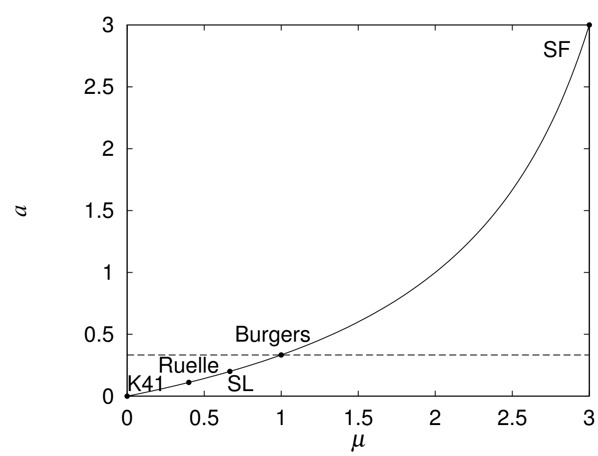

FIG. 1: The a-μ diagram, with relationship $a = \frac{\mu}{4-\mu}$. The horizontal line denotes $a = 1/3$.

D. A constraint on the scaling exponents

We derive one constraint on the p-th order scaling exponents ζ_p for the velocity structure function

$$\langle (\delta u_r)^p \rangle \propto r^{\zeta_p},$$

where the brackets denote an ensemble average.

Again, by 1),

$$\epsilon = 2\nu \int_0^{k_d} k^2 E(k) dk$$

is independent of ν in the limit $\nu \to 0$. Because k_d is related with the L^∞-norm of the velocity gradient and $E(k)$ with the L^2-norm, it should give a constraint on ζ_p, We will determine what this is.

By the definition

$$\left\langle \left(\frac{\delta u_r}{r} \right)^p \right\rangle^{\frac{1}{p}} \propto r^{\frac{\zeta_p}{p}-1},$$

we have

$$\|\nabla \boldsymbol{u}\|_{L^p} = \lim_{r \to r_{\min}} \left\langle \left(\frac{\delta u_r}{r} \right)^p \right\rangle^{\frac{1}{p}} \propto \nu^{\frac{3(a+1)}{4}\left(\frac{\zeta_p}{p}-1\right)}$$

and [43]

$$\|\nabla \boldsymbol{u}\|_{L^\infty} = \lim_{p \to \infty} \lim_{r \to r_{\min}} \left\langle \left(\frac{\delta u_r}{r} \right)^p \right\rangle^{\frac{1}{p}} \propto \nu^{\frac{3(a+1)}{4}(\alpha-1)}, \tag{23}$$

where $\alpha \equiv \lim_{p\to\infty} \frac{\zeta_p}{p}$ is finite by 2) [44]. Here we essentially make use of the regularity of the Navier-Stokes solutions. An asymptotic linearity of ζ_p follows from the finiteness of α. In fact, we can obtain a more precise expression for the exponents.

By (23) and $(20)_1$, we find in the limit of $\nu \to 0$

$$\alpha = \frac{1-3a}{3(1+a)}. \tag{24}$$

(Note that $a = \dfrac{1-3\alpha}{3(1+\alpha)}$, hence the inverse has the same functional form.) Because of $E(k) \propto k^{-q}$ and (17) and the definition $q = 1 + \zeta_2$, we also have

$$\zeta_2 + 1 = \frac{5+9a}{3(1+a)}. \tag{25}$$

Eliminating a between (24) and (25), we obtain

$$\zeta_2 + \lim_{p\to\infty} \frac{\zeta_p}{p} = 1. \tag{26}$$

Up to here, fractal nature of energy cascade such as in the β-model is *not* assumed. The condition (26) implies

$$\zeta_p = (1-\zeta_2)p + o(p) \tag{27}$$

for large p. A super-linear behavior in ζ_p, as in the log-normal model, is thus excluded by the finiteness of α. In other words, this argument supports an asymptotic linear behavior of the scaling exponent predicted in the β-model[45]. In the framework of multi-fractal theory for turbulence we may relate $1-\zeta_2 = h_{\min}$, where $h_{\min}$ is the minimum possible scaling exponent, see e.g. [46]. In two-dimensional turbulence, the scaling exponents have bounds as a result of vorticity conservation in the inviscid limit [47]. See also [48] for 'asymptotic linearization' of scaling exponents in more general cases.

A simple inequality for ζ_p follows from this. Setting

$$\zeta_p = (1-\zeta_2)p + f_p, \quad \text{with} \quad \lim_{p\to\infty} f_p = 0,$$

we have $f_3 = 1 - 3(1-\zeta_2)$ by $\zeta_3 = 1$. By the convexity $f_p \le f_3$ for $p \ge 3$, we find

$$\zeta_p \le (1-\zeta_2)(p-3) + 1. \tag{28}$$

We note that the prediction from the β-model

$$\zeta_p = \frac{p}{3} - \frac{\mu}{3}(p-3)$$

satisfies (26) for arbitrary $\mu(>0)$, that is, we *cannot* fix μ by the constraint (26), as it becomes an identity.

If $\zeta_2 = \frac{2}{3}$, (28) implies that

$$\zeta_p \le \frac{p}{3}, \quad \text{for any} \quad p \ge 3.$$

On the other hand, if $\zeta_2 = \frac{\mu+2}{3}$, we would have

$$\zeta_p \le \frac{p}{3} - \frac{\mu}{3}(p-3),$$

which means (28) places the β-model as an upper-bound of the possible scaling.

It should be noted that all the above results are obtained by balancing powers of ν, hence the arguments are valid only in the limit of $\nu \to 0$. For finite Reynolds number turbulence, (28) would not hold as is.

Remark: By a rigorous analysis in [40] we have instead $q \le \dfrac{5+9a}{3(1+a)}$ (see Appendix A), this leads to

$$\zeta_2 + \lim_{p\to\infty} \frac{\zeta_p}{p} \le 1.$$

It can also be obtained by writing (28)

$$1-\zeta_2 \ge \frac{\zeta_p - 1}{p-3} \text{ for } p > 3$$

and passing to the limit $p \to \infty$. See also [49–52] for mathematical works on intermittency.

III. NUMERICAL EXPERIMENTS

A. Numerical Methods

The pseudo-spectral method was used for the evaluation of nonlinear terms and the fourth-order Runge-Kutta for time-stepping. The initial data are generated with the energy spectrum

$$E(k) = k^4 e^{-k^2}, \tag{29}$$

where the phases of the Fourier coefficients are randomized.

The numerical simulations have been performed for various values of Reynolds number by choosing the number of grid points N, and viscosity ν to ensure that the turbulence is developed and resolved. Results were obtained from a $N = 256$ cubic grid, with mesh size $\Delta x = 2\pi/N$ and time increment $\Delta t = 2 \times 10^{-3}$. Typically, in the case of forced simulations, we have as an estimate of accuracy $k_{\max}\eta \ge 1.5$ for $\nu = 0.005$ and $k_{\max}\eta \ge 1.1$ for $\nu = 0.0025$ throughout the time evolution. For the latter (slightly under-resolved) case a check was performed with a $N = 512$ cubic grid to ensure agreement, and hence that none of our results are numerical artifacts.

The integral $\delta(r)$ is calculated for a sequence of values of r, increasing outwards from the center point $\boldsymbol{x}_0$ of the spatial integration region. The increasing radii of integration are taken as

$$r_j = \frac{2\pi d^{j-1}}{N}, \quad \text{for } j = 1, 2, 3, ..., p, \tag{30}$$

to determine the power-law relationship between $\delta(r)$ and r. The fundamental period is 2π, and $d > 1$ is chosen such that the sphere at r_p covers at least 10% of the total spatial range 2π.

By monitoring the time-evolution of the energy and the enstrophy, the lower limit of the time integral t_0 is set after the turbulence reaches a statistically steady state. The time integral is taken over the range $t_0 < t < t_0 + r^2/\nu$. The quantity $\delta(r)$ was calculated for various different center points in order to determine the effect of position. These points were chosen, some at fixed $(0, 0, 0)$, $(\pi, 0, 0)$, $(0, \pi, 0)$, $(\pi, \pi, 0)$, and others at points of local (in space and time) maxima of $|\nabla \boldsymbol{u}|^2$.

Two important quantities are $E(t) = \frac{1}{2}\langle|\boldsymbol{u}|^2\rangle$ and $Q(t) = \frac{1}{2}\langle|\boldsymbol{\omega}|^2\rangle$, which denote the spatial average of kinetic energy and the enstrophy, respectively.

B. Freely-decaying case

We first study freely-decaying turbulence. In this case we take t_0 after the time corresponding to the peak enstrophy as this is the point at which turbulence begins to decay [29]. The parameter d is chosen to be 1.92.

Because the Reynolds number is not sufficiently large, the energy spectrum does not display the characteristic Kolmogorov power-law for fully-developed turbulence [26, 28] for sufficiently long time to evaluate the space-time integral accurately. This can be seen in Fig.2, which shows a log-log plot of the energy spectra as a function of the wavenumber for various times throughout the time range covered by the integral. Figure 3 shows the evolution of the enstrophy, for the two values of viscosity throughout this time interval.

In Fig.4 we show local Reynolds number $\delta(r)$ against r. Due to the rapid decay of energy mentioned earlier, a clear power-law behavior is not observed. Nevertheless we do observe an r^4 behavior for small r and a shallower power-law for larger r.

C. Forced Turbulence

To integrate $\delta(r)$ for a sufficiently long time to ensure its convergence, we introduce a forcing term. At every time step, the vorticity components for wavenumber $|\boldsymbol{k}| = 1$, are held fixed at their initial values, effectively injecting energy back into the system and sustaining a statistically steady state of turbulence. As can be seen from Fig.5, the energy spectra display a power-law close to $-5/3$, corresponding to the Kolmogorov spectrum in turbulence. This persists throughout the whole time interval required for the evaluation

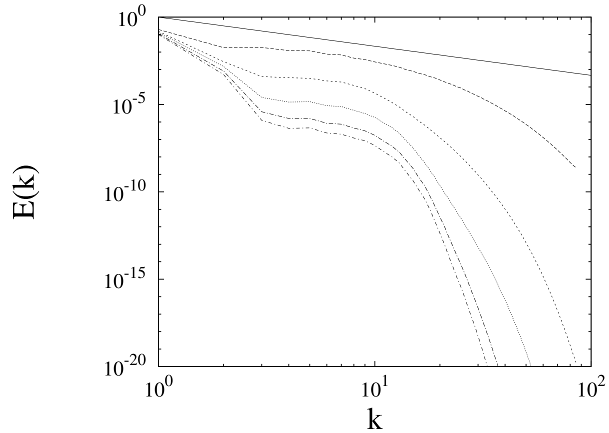

FIG. 2: The energy spectra for the freely-decaying case with $\nu = 5 \times 10^{-3}$: the upper to lower dashed lines show spectra for $t = 10, 30, 50, 70$ and 86, respectively. The solid line represents a slope $k^{-5/3}$.

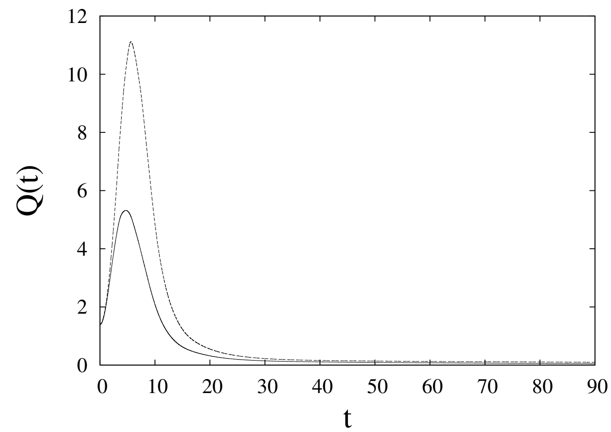

FIG. 3: Evolution of the enstrophy for the freely-decaying case with $\nu = 5\times10^{-3}$ (solid) and $\nu = 2.5 \times 10^{-3}$ (dashed).

of the space-time integral. Figure 6 shows the evolution of enstrophy associated with this forced computation. At first, we see an increase up to a maximum, it then levels out into a statistically steady state, which fluctuates about an average value. Figure 7 is shown to verify that the dissipation rate $\epsilon(t)$ is independent of ν. We can then calculate the Kolmogorov length scale based on the time average of the enstrophy in each case of viscosity, using $\eta = (\nu^3/\epsilon)^{1/4} = 1/k_d$, where $\epsilon = 2\nu\overline{Q}$ is the time-averaged energy dissipation rate. It is $\eta \approx 2.2 \times 10^{-2}$ for $\nu = 5 \times 10^{-3}$, and $\eta \approx 1.3 \times 10^{-2}$ for $\nu = 2.5 \times 10^{-3}$. For these forced computations, Taylor microscale Reynolds number $R_\lambda = \sqrt{\frac{10}{3}\frac{E}{\nu\sqrt{Q}}}$. is about 70 for $\nu = 0.005$ and 120 for $\nu = 0.0025$. The estimates of η, corresponding to the values of viscosity, are indicated by an arrow on Figs.8 and 9.

This statistically steady state produces a clearer power-law behavior. The integral was evaluated at different center points, for two different values of viscosity and $d = 1.92$. The double-log plots of $\delta(r)$ with r^4 for each viscosity are shown in Figs.8 and 9. At least at this moderately high Reynolds number, the function $\delta(r)$ displays a clear power-law $\delta(r) \propto r^4$ throughout the inertial subrange. As noted above this is expected only in the dissipative range.

Then why do we have $\delta(r) \propto r^4$ in the whole the inertial subrange ? To explain this,

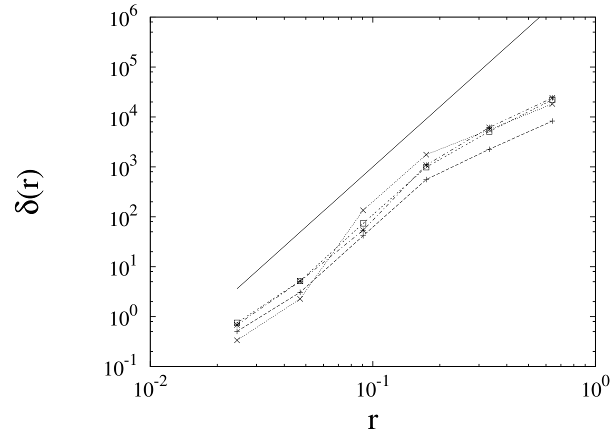

FIG. 4: The CKN integral $\delta(r)$ against r for various center points, compared with r^4 (solid) for $\nu = 5 \times 10^{-3}$. Line conventions are $\boldsymbol{x}_0 = (0,0,0); +,\ (\pi,0,0); \times,\ (0,\pi,0); *,\ (\pi,\pi,0); \Box$.

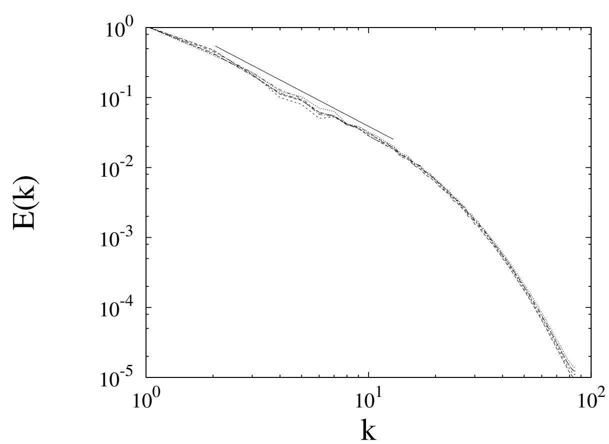

FIG. 5: Energy spectra for the forced case: $\nu = 2.5 \times 10^{-3}$ compared with $k^{-5/3}$ (solid), the dashed lines show spectra for times $10, 30, 50, 70$ and 90, respectively.

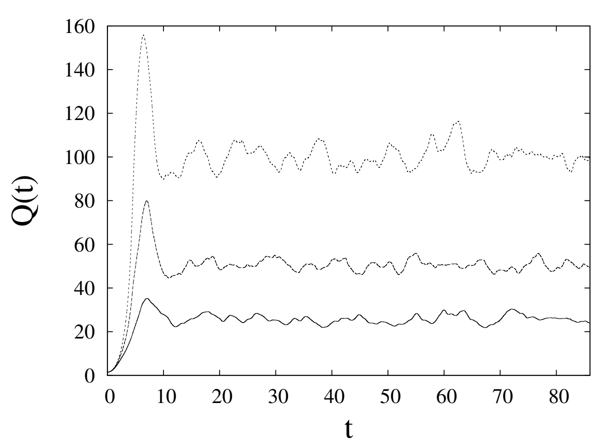

FIG. 6: Time evolution of the enstrophy for the forced case: $\nu = 1 \times 10^{-2}$ (solid), 5×10^{-3} (dashed) and 2.5×10^{-3} (dotted).

.

we compare in Fig.10, the time evolution of r_* with those of the Taylor micro-scale $\lambda(t) = \sqrt{10\nu E(t)/\epsilon(t)}$, and the Kolmogorov scale $\eta(t) = (\nu^3/\epsilon(t))^{1/3}$, where $\epsilon(t) = 2\nu Q(t)$. Also

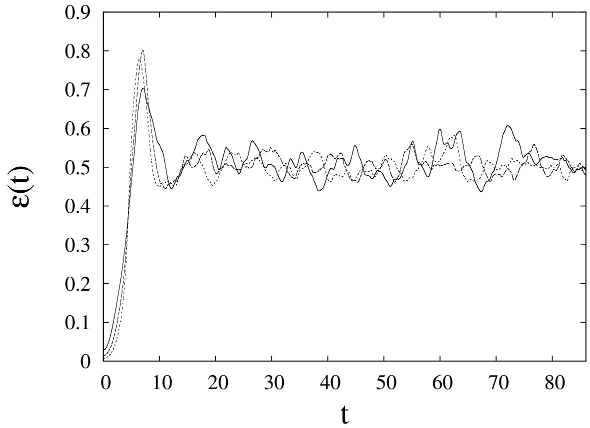

FIG. 7: Time evolution of the energy dissipation rate for the forced case. The plot shows the independence of $\epsilon(t)$ and ν. Line convention is the same as in Fig 6.

plotted is the integral scale $L(t)$ defined by

$$L(t) = \frac{3\pi}{4E(t)} \int_0^\infty k^{-1} E(k,t) dk.$$

It is clear that they are very different; $r_* \approx 1$ takes a value which is a multiple of λ and it is larger than η by almost two orders-of-magnitude. It should be noted that the cross-over scale lies close to the energy-containing range, whose characteristic scale is $L(t) \approx 1.5$. This makes a marked contrast to the exact solutions of Burgers vortex and equations, where r_* lies in the dissipative scale. (See Section IV below.)

To study its behavior more precisely, we show the time-averaged r_* for various values of ν in Fig.11. (The original definition $r_*/L = \overline{\left(\frac{3}{4\pi}\frac{\epsilon(t)}{\nu\|\nabla \boldsymbol{u}\|_\infty}\right)^{1/3}}$ is used for its evaluation here, but no change is observed even if we take time-average $\overline{\epsilon(t)}$ first .) It shows that r_* shows a power-law dependence on ν with a small exponent, that is, $r_* \propto \nu^a$ with $a \approx 0.26$. More importantly, $r_* = O(1)$ in the energy-containing range for all the values of ν used. This is why we do not observe a transition to $\delta(r) \propto r$ within the inertial subrange.

We have noted above that ζ_p behaves linearly at large p just like the β-model. If the β-model is perfectly correct that would imply the dissipation correlation exponent $\mu(= 3 - D)$ takes $\mu = \frac{4a}{1+a} \approx 0.8$, which is much larger than the experimentally accepted range 0.2-0.4. Indeed, we see in Fig.12 that the dissipation correlation has $\mu = 0.20$. This means that while the β model is not valid quantitatively, it remains valid qualitatively. For experimental works on dissipation correlation and intermittency, see [53–55] and more recent [56–61].

In an attempt to find a more singular behavior, that is, $\delta(r) \propto r^n$ with $n < 4$, we have also computed a flow form of colliding orthogonal Lamb dipoles [62, 63]. The motivation was to locate the point $(\boldsymbol{x_0}, t_0)$ in a region where intense vorticity is formed. It turns out, however, that such a point moves in space significantly and we could not observe a clear power-law behavior, although a general trend of decreasing exponent in $\delta(r)$ as r increases was still seen (figure omitted).

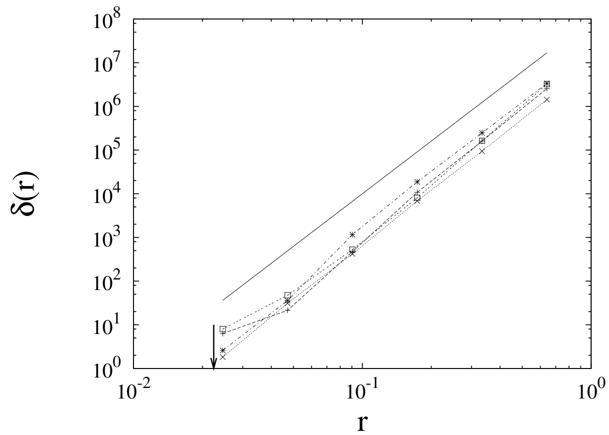

FIG. 8: The CKN integral $\delta(r)$ vs. r for various center points, compared with r^4 (solid) for $\nu = 5 \times 10^{-3}$. Line convention is the same as in Fig.4. The arrow indicates the Kolmogorov length scale η.

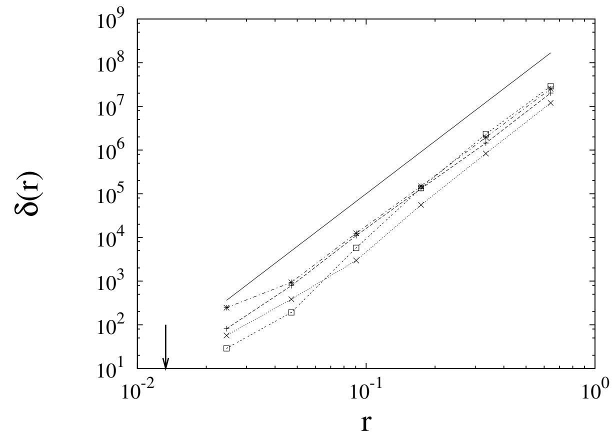

FIG. 9: The CKN integral $\delta(r)$ vs. r for various center points, compared with r^4 (solid) for $\nu = 2.5 \times 10^{-3}$. Line convention is the same as in Fig.4. The arrow indicates the Kolmogorov length scale η.

IV. EXAMPLES BY EXACT SOLUTIONS

Fluid turbulence is known to be a multi-scale phenomenon. In this section, for comparison we work out the function $\delta(r)$ on the basis of exact solutions, which represent single-scale phenomena.

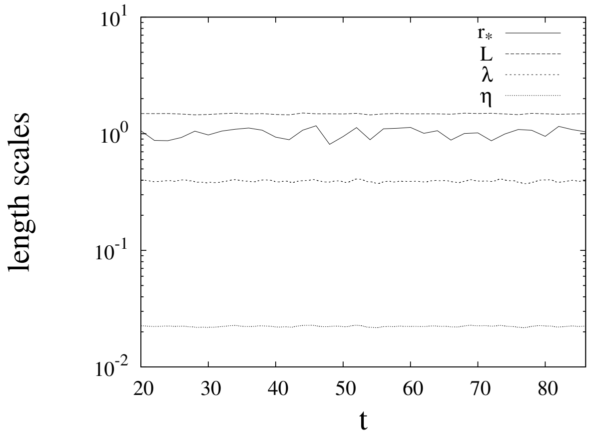

FIG. 10: Time evolution of r_* (solid) together with that of the Taylor micro-scale $\lambda(t)$ (dashed) and the Kolmogorov length scale $\eta(t)$ (dotted) for $\nu = 0.005$. Also shown is the integral scale $L(t)$.

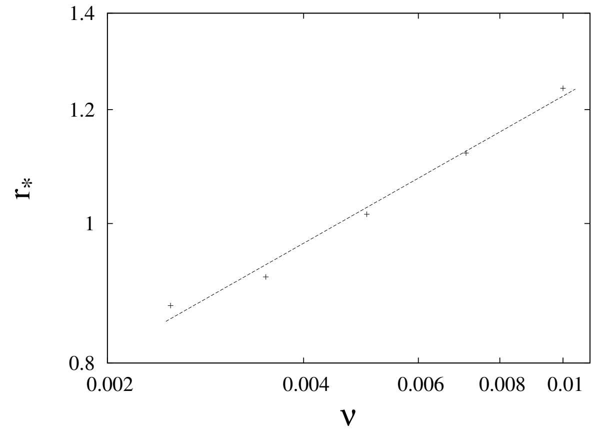

FIG. 11: The cross-over scale r_* as a function of viscosity: $r_* \propto \nu^a$. The straight line shows a least-squares fit with $a = 0.26$.

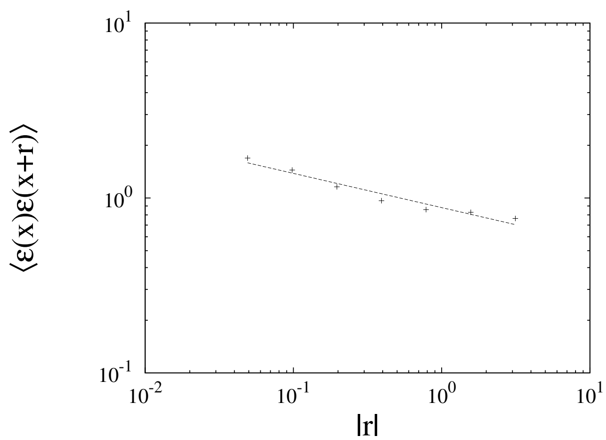

FIG. 12: The dissipation correlation $\langle \epsilon(\boldsymbol{x})\epsilon(\boldsymbol{x}+\boldsymbol{r})\rangle \propto |\boldsymbol{r}|^{-\mu}$ with a least-squares fit $\mu = 0.20$.

A. Burgers Vortex

We consider the Burgers vortex, an exact solution of the Navier-Stokes equations subject to a constant straining flow. The velocity for the Burgers vortex tube in cylindrical polar coordinates is given by

$$\begin{cases} u_r = -\alpha r, \\ u_\theta = \frac{\Gamma}{2\pi r}\left(1 - e^{-\frac{\alpha r^2}{2\nu}}\right), \\ u_z = 2\alpha z, \end{cases} \tag{31}$$

and the vorticity by

$$\omega = \frac{\alpha\Gamma}{2\pi\nu} \exp\left(-\frac{\alpha r^2}{2\nu}\right).$$

Here, the constant α denotes rate of strain and Γ velocity circulation. It can be shown that

$$|\nabla \boldsymbol{u}|^2 = 6\alpha^2 + \left(\frac{\partial u_\theta}{\partial r}\right)^2 + \left(\frac{u_\theta}{r}\right)^2, \tag{32}$$

see e.g. [4]. The definition of $\delta(r)$ is similar to the one in previous section. In this case, the integral to be calculated is

$$\delta(r) = \frac{1}{\nu}\int_{Q_r^{2D}} |\nabla \boldsymbol{u}|^2 \, d\boldsymbol{x} \, dt. \tag{33}$$

The bounds of Q_r^{2D} are given by $|\boldsymbol{x} - \boldsymbol{x}_0| < r$ and $|t - t_0| < r^2/\nu$, where $\boldsymbol{x} = (x, y)$. Because this is a steady state solution, the time integral simplifies to a multiplication by r^2/ν [29], we have

$$\delta(r) = \frac{r^2}{\nu^2}\int_{V_r^{2D}} |\nabla \boldsymbol{u}|^2 \, d\boldsymbol{x}, \tag{34}$$

where V_r^{2D} denotes a disc of radius r. Noting that as $r \to 0$,

$$\frac{1}{|V_r^{2D}|}\int_{V_r^{2D}} |\nabla \boldsymbol{u}|^2 \, d\boldsymbol{x} \to |\nabla \boldsymbol{u}|^2(\boldsymbol{x}_0),$$

with $|V_r^{2D}| = \pi r^2$, we have

$$\delta(r) \to \begin{cases} \pi\frac{r^4}{\nu^2}|\nabla \boldsymbol{u}|^2(\boldsymbol{x}_0) & \text{as } r \to 0, \\ \frac{r^2}{\nu^2}\int_{\mathbb{R}^2} |\nabla \boldsymbol{u}|^2 d\boldsymbol{x} & \text{as } r \to \infty. \end{cases} \tag{35}$$

The cross-over takes place at $r = r_*$, where

$$\frac{r^4}{\nu^2}|\nabla \boldsymbol{u}|^2(\boldsymbol{x}_0) \approx \frac{r^2}{\nu^2}\int_{\mathbb{R}^2} |\nabla \boldsymbol{u}|^2 d\boldsymbol{x},$$

or,

$$r_* = \left(\frac{\int_{\mathbb{R}^2} |\nabla \boldsymbol{u}|^2 d\boldsymbol{x}}{|\nabla \boldsymbol{u}|^2(\boldsymbol{x}_0)}\right)^{1/2}.$$

Using $|\nabla \boldsymbol{u}|^2 \approx \omega^2 \approx \left(\frac{\alpha\Gamma}{2\pi\nu}\right)^2$ and $\epsilon = \nu\int_{\mathbb{R}^2} |\nabla \boldsymbol{u}|^2 d\boldsymbol{x} \approx \frac{\alpha\Gamma^2}{4\pi}$, we find

$$r_* \approx \left(\frac{\pi\nu}{\alpha}\right)^{1/2}.$$

This is proportional to the core radius of the Burgers vortex.

We can confirm this result by using the exact solution. In the limit of large Reynolds number, $r/\nu \gg 1$, we may neglect the first term on the right hand side of (32). The spatial part of the integral becomes

$$\frac{1}{\nu}\int_0^r |\nabla \boldsymbol{u}|^2\, 2\pi r\, dr \simeq \frac{2\pi}{\alpha}\left(\frac{\alpha\Gamma}{4\pi\nu}\right)^2 \int_0^{\frac{\alpha r^2}{2\nu}} \left[\left(2e^{-\xi} - \frac{1-e^{-\xi}}{\xi}\right)^2 + \left(\frac{1-e^{-\xi}}{\xi}\right)^2\right] d\xi, \tag{36}$$

where $\xi = \alpha r^2/2\nu$ [4]. It follows that

$$\int_0^r |\nabla \boldsymbol{u}|^2\, 2\pi r\, dr \to \begin{cases} r^2|\nabla \boldsymbol{u}|^2 & \text{for } r \ll \sqrt{\nu/\alpha}, \\ \int_{\mathbb{R}^2} |\nabla \boldsymbol{u}|^2 d\boldsymbol{x} & \text{for } r \gg \sqrt{\nu/\alpha}. \end{cases} \tag{37}$$

This confirms the transition at $r \approx \sqrt{\nu/\alpha}$ and we have as $r \to 0$

$$\delta(r) \propto \frac{1}{\pi}\left(\frac{\Gamma}{\nu}\right)^2 \xi^2,$$

which is consistent with the above $\delta(r) \propto r^4$. We note that in this case r_* lies in the dissipation range; $r_* \propto \nu^{1/2}$. Unlike Navier-Stokes turbulence, a typical multi-scale phenomenon, this example has a single scale.

B. Burgers equation

As another example, we consider the Burgers equation

$$\frac{\partial u}{\partial t} + u\frac{\partial u}{\partial x} = \nu\frac{\partial^2 u}{\partial x^2}. \tag{38}$$

As a comparison, we compute $\delta(r)$, which in one dimension is given by;

$$\delta(r) = \frac{r}{\nu}\int_{Q_r^{1D}} \left(\frac{\partial u}{\partial x}\right)^2 dx\, dt, \quad Q_r^{1D}(x,t) = \left\{(x,t) : |x - x_0| < r,\, t_{\max} - \frac{r^2}{\nu} < t < t_{\max}\right\}. \tag{39}$$

The power-law can be worked out by a simple analysis for

$$\delta(r) = \frac{r^3}{\nu^2}\int_{Q_r^{1D}} \left(\frac{\partial u}{\partial x}\right)^2 dx. \tag{40}$$

In the limit $r \to 0$ the integral scales as $\propto r(\partial u/\partial x)^2$, and we have

$$\delta(r) \propto \begin{cases} 2\frac{r^4}{\nu^2}\left(\frac{\partial u}{\partial x}\right)^2 & \text{as} \quad r \to 0, \\ \frac{r^3}{\nu^2}\int_{-\infty}^{\infty}\left(\frac{\partial u}{\partial x}\right)^2 dx & \text{as} \quad r \to \infty \end{cases} \tag{41}$$

The cross-over occurs at

$$r_* = \frac{\int_{-\infty}^{\infty} \left(\frac{\partial u}{\partial x}\right)^2 dx}{2 \sup_x \left(\frac{\partial u}{\partial x}\right)^2}.$$

An exact steadily traveling wave solution can be written as

$$u = U \tanh \frac{Ux}{2\nu},$$

after a translation. For this solution, we have $\frac{\partial u}{\partial x} = \frac{U^2}{2\nu}\mathrm{sech}^2 \frac{Ux}{2\nu}$ and $\int_{-\infty}^{\infty} \left(\frac{\partial u}{\partial x}\right)^2 dx = \frac{2U^3}{3\nu}$, thus we find

$$r_* = \frac{4}{3U}\nu.$$

The cross-over scale is on the order of the width of the shock wave. Again, r_* is in the dissipative range unlike for the Navier-Stokes flows; $r_* \propto \nu^1$.

We can confirm this by the exact solution. It gives in this case

$$\delta(r) = 4\xi^3 \left(\tanh \xi - \frac{1}{3}\tanh^3 \xi\right),$$

where $\xi = \frac{Ur}{2\nu}$. It follows that

$$\delta(r) \approx 4\xi^4 \text{ as } \xi \to 0,$$

in agreement with the above analysis.

A pseudo-spectral calculation was performed in a way analogous to that of the three-dimensional case, starting from initial data $u_0 = \sin x$, with $x_0 = \pi$ located at the position of shock wave formation for the velocity field. The scaling of $\delta(r)$ is close to r^4 for small r and becomes closer to a shallower r^3 as r increases, consistent with the above argument (figure omitted).

V. SUMMARY AND DISCUSSION

Intermittency in turbulence is related with the mathematical problem of the Navier-Stokes equations in that it is associated with rapid growth of local vorticity. By using the CKN local Reynolds number, we have developed a systematic method of characterization of intermittency.

First, we have re-examined the CKN integral and identified a cross-over scale r_*, at which the scaling behavior of $\delta(r)$ changes. On this basis, we have introduced the parameter a

characterizing intermittency as $r_* \propto \nu^a$. As a by-product we have derived the constraint $\lim_{p\to\infty} \frac{\zeta_p}{p} = 1 - \zeta_2$ for the scaling exponents ζ_p of the velocity structure functions in the limit $\nu \to 0$. This in turn implies that $\zeta_p = (1-\zeta_2)p + o(p)$.

Second, we have performed direct numerical simulations of the Navier-Stokes equations at moderately high Reynolds numbers (≈ 100) to examine the behavior of the CKN integral $\delta(r)$. We have found a scaling $\delta(r) \propto r^4$ in the whole inertial range, not only in the dissipative range. We explain the absence of cross-over phenomenon by finding r_* is actually in the energy-containing range. The intermittency parameter a is found to be 0.26. If the β-model is perfectly correct, $a = 0.26$ would imply $\mu = 0.8$ for the dissipation correlation exponent, which is beyond the acceptable range. We point out that while the β-model is not quantitatively perfect, but its prediction serves as an upper-bound for the scaling exponents. Similar cross-over phenomena have been studied on the basis of exact solutions of the Burgers vortex and the Burgers equation.

By the definition of the cross-over scale (10) and $r_* \propto \nu^a$, for stronger intermittency with larger a, near-singular structures are captured better by the L^∞-norm which is more sensitive than the L^2-norm. If we make ν smaller in higher Reynolds number computations, r_* will be shifted to smaller values assuming that a remains unchanged. It might be possible to observe the transition, as was noted to be the case for the 1D Burgers equation with $r_* \propto \nu^1$. Such studies with higher Reynolds number will be left for future study.

All the results obtained here are based on the framework of phenomenology, but we have double-checked their consistency against rigorous mathematical theory, where possible e.g. [36, 40]. It would be interesting to make the present theory solid, say, by applying Besov-space techniques. This will also be left for future study.

Acknowledgments

This work has been supported by an EPSRC Grant No. EP/F009267/1. One of the authors (K.O.) has also been supported by Royal Society Wolfson Research Merit Award. He also thanks L. Chevillard, C. Doering, J. Gibbon, Y. Li and A. Willis for discussion and T. Matsumoto for useful comments.

APPENDIX A: RELATION TO DOERING-GIBBON BOUNDS

Notations in this section are the same as those of [40].

As seen above, we have $\|\nabla \boldsymbol{u}\|_\infty \approx Re^{(1+3a)/2}$ for $r_* \propto \nu^a$. It follows that $\left\langle \kappa_{n,1}^2 \right\rangle \leq c_n L^{-2} Re^{\frac{3}{2}(a+1)}$, where $Re \propto 1/\nu$. Then we have

$$\begin{aligned}\left\langle \kappa_n^2 \right\rangle &\leq Re^{\frac{3}{2}(a+1)\frac{n-1}{n}} Re^{\frac{1}{n}} \\ &= Re^{\frac{3}{2}(a+1)-\frac{3a+1}{2n}},\end{aligned}$$

in place of (78) and (79) of [40]. Using Lemma 1 of [40], we find

$$L^{2n} \left\langle \kappa_n^2 \right\rangle^n \leq c_n Re^{\frac{3}{2}(a+1)n-\frac{3a+1}{2}},$$

or

$$L \left\langle \kappa_n \right\rangle \leq c_n Re^{\frac{3}{4}(a+1)-\frac{3a+1}{4n}}.$$

Comparing this with $Re^{\frac{1}{3-q}-\frac{1}{2n}\frac{q-1}{3-q}}$, we get

$$q \leq \frac{5+9a}{3(a+1)} = \frac{5}{3} + \frac{4a}{3(1+a)}$$

for the exponent of the energy spectrum $E(k) \approx k^{-q}$.

APPENDIX B: LOG-POISSON MODEL

The Log-Poisson model has

$$\zeta_p = \frac{p}{9} + 2\left(1 - \left(\frac{2}{3}\right)^{p/3}\right)$$

for the scaling exponents. It follows that

$$\alpha = \lim_{p\to\infty} \frac{\zeta_p}{p} = 1/9 \approx 0.111,$$

and

$$1 - \zeta_2 = 2\left(\frac{2}{3}\right)^{\frac{2}{3}} - \frac{11}{9} \approx 0.304 \neq \lim_{p\to\infty} \frac{\zeta_p}{p}.$$

This model is thus not consistent with the fundamental constraint (26).

Equivalently, in terms of $E(k) \propto k^{-q}$, $a = \frac{1-3\alpha}{3(1+\alpha)} = 1/5$ implies $q = \frac{5+9a}{3(1+a)} = \frac{17}{9} \approx 1.888$, whereas actually it has $\zeta_2 + 1 = \frac{29}{9} - 2\left(\frac{2}{3}\right)^{2/3} \approx 1.6959$.

---

[1] C.R. Doering, "The 3D Navier-Stokes problem," Annu. Rev. Fluid Mech. **41**, 109 (2009).

[2] C.R. Doering and J.D. Gibbon, *Applied Analysis of the Navier-Stokes Equations,* (Cambridge University Press, Cambridge, 1995).

[3] J.D. Gibbon, 'Regularity and singularity in solutions of the three-dimensional Navier-Stokes equations," Proc. Roy. Soc. A **466**, 2587(2010).

[4] K. Ohkitani, "A miscellany of basic issues on incompressible fluid equations," Nonlinearity. **21**, 255 (2008).

[5] C. Foias, O. Manley, R. Rosa and R. Temam *Navier-Stokes Equations and Turbulence,* Cambridge, Cambridge University Press, 2001.

[6] J. Leray, "Essai sur le mouvement d'un liquide visqueux emplissant l'espace," Acta Math. **63**, 193 (1934). English translation: `http://www.math.cornell.edu/~bterrell/leray.html`.

[7] E. Hopf, "On the initial value problem for the basic equations of hydrodynamics," Math. Nachr. **4**, 213 (1951). English translation: `http://www.dam.brown.edu/people/menon/am224/hopf-NS.pdf`.

[8] V. Scheffer, "Hausdorff measure and the Navier-Stokes equations," Commun. Math. Phys. **55**, 97 (1977).

[9] L. Caffarelli, R. Kohn, and L. Nirenberg., "Partial regularity of suitable weak solutions of the Navier-Stokes equations," Commun. Pur. Appl. Math. **35**, 771 (1982).

[10] E. Kim, H. Liu and J. Anderson, "Intermittency and self-organization in turbulent flows," Phys. Scripta, **142** 014053 (2010).

[11] M. Arnold and W. Craig, "On the size of the Navier-Stokes singular set," Discret. Contin. Dyn. S. **28**, 1165 (2010).

[12] S.I. Chernyshenko, P. Constantin, J.C. Robinson and E.S. Titi, "A posteriori regularity of the three-dimensional Navier-Stokes equations from numerical computations," J. Math. Phys. **48**, 065204 (2007).

[13] A. Pumir and E. D. Siggia, "Incipient singularities in the Navier-Stokes equations," Phys. Rev. Lett. **55**, 1749 (1985)

[14] A. Pumir and E. D. Siggia, "Vortex dynamics and the existence of solutions to the Navier-Stokes equations," Phys. Fluids. **30**, 1606 (1987)

[15] A. Pumir and E. D. Siggia, "Finite-time singularities in the axisymmetric three-dimension Euler equations," Phys. Rev. Lett. **68**, 1511 (1992)

[16] J. Schumacher, B. Eckhardt and C. Doering, "Extreme vorticity growth in Navier-Stokes

turbulence," Phys. Lett. A **374**, 861 (2010).

[17] L. Lu and C.R. Doering, "Limits on enstrophy growth for solutions of the three-dimensional Navier-Stokes equations," Indiana U. Math. J. **57**, 2693 (2008).

[18] K. R. Sreenivasan and C. Meneveau, "Singularities of the equations of fluid motion," Phys. Rev. A **38**, 6287 (1988).

[19] T. Y. Hou, Z. Lei and C. Li, "Global regularity of the 3D axi-symmetric Navier-Stokes equations with anisotropic data," Commun. Part. Diff. Eq.**33**, 1622 (2008).

[20] T. Y. Hou and Z. Lei, "On the partial regularity of a 3D model of the Navier-Stokes equations," Commun. Math. Phys. **287**, 589 (2009).

[21] T. Y. Hou, C. Li, Z. Shi, S. Wang and X. Yu. "On singularity formation of a nonlinear nonlocal system," Arch. Rational Mech. Anal. **199**, 117 (2011).

[22] P. E. Hamlington, J. Schumacher and J. A. Dahm, "Local and nonlocal strain rate fields and vorticity alignment in turbulent flows," Phys. Rev. E **77**, 026303(2008).

[23] P. E. Hamlington, J. Schumacher, J. A. Dahm, "Direct assessment of vorticity alignment with local and nonlocal strain rates in turbulent flows," Phys. Fluids. **20**, 111703(2008).

[24] C. L. Fefferman, *The Millennium Prize Problems* (American Mathematical Society, Providence, RI, 2006), pp. 57-70.

[25] J. G. Heywood, "Remarks on the possible global regularity of solutions of the three-dimensional Navier-Stokes equations," Pitman Res. Notes Math. Ser. **308**, 1 (1994).

[26] A. Biryuk and W. Craig, "Bounds on Kolmogorov spectra for the Navier-Stokes equations," Physica D **241**, 426 (2012).

[27] B. B. Mandlebrot, "On the geometry of homogeneous turbulence, with stress on the fractal dimension of the iso-surfaces of scalars", J. Fluid Mech. **72**, 401 (1975).

[28] H. A. Rose and P. L. Sulem, "Fully developed turbulence and statistical mechanics," J. Phys. (Paris) **39**, 441 (1978).

[29] G. Gallavotti, "Some rigorous results about 3D Navier-Stokes," in Les Houches 1992 NATO-ASI meeting on "Turbulence in Extended Systems," eds. R. Benzi, C. Basdevant and S. Ciliberto (Nova Science, New York, 1993) 45.

[30] G. Gallavotti, *Foundations of Fluid Dynamics* (Springer, Berlin, 2002).

[31] K. Ohkitani and M. Dowker "Numerical study on comparison of Navier-Stokes and Burgers equations", Phys. Fluids **24**, 055133(2012).

[32] J.C. Robinson, and W. Sadowski, “Decay of weak solutions and the singular set of the three-dimensional Navier-Stokes equations,” Nonlinearity, **20**, 1185(2007).

[33] I. Kukavica, “The fractal dimension of the singular set for solutions of the Navier-Stokes system,” Nonlinearity, **22**, 2889(2009).

[34] P.L. Sulem and U. Frisch, “Bounds on energy flux for finite energy turbulence,” J. Fluid Mech, **72**, 417 (1975).

[35] W.D. Henshaw, H.O. Kreiss and L.G Reyna, ”Smallest scale estimates for the Navier-Stokes equations for incompressible fluids,” Arch. Rat. Mech. Anal. **112**, 21 (1990).

[36] W.D. Henshaw, L.G Reyna and H.O. Kreiss, ”On the smallest scale for the incompressible Navier-Stokes equations,” Theor. Comput. Fluid Dyn. **1**, 65 (1989).

[37] G. Paladin and G. Vulpiani, “Degrees of freedom of turbulence,” Phys. Rev. A **35**, 1971(1987).

[38] U. Frisch, P.L. Sulem and M. Nelkin, “A simple dynamical model of intermittent fully developed turbulence,” J. Fluid Mech, **87**, 719 (1978).

[39] D. Ruelle, “Large volume limit of the distribution of characteristic exponents in turbulence,” Commun. Math. Phys. **87**, 287(1982)

[40] C.R. Doering and J.D. Gibbon, “Bounds on moments of the energy spectrum for weak solutions of the three-dimensional Navier-Stokes equations,” Physica D. **165**, 163(2002).

[41] Z.S. She and E. Leveque, “Universal scaling laws in fully developed turbulence,” Phys. Rev. Lett. **72**, 336(1994).

[42] J. Schumacher, K.R. Sreenivasan,and V. Yakhot, “Asymptotic exponents from low-Reynolds-number flows” New J. Phys. **9**, 89(2007).

[43] In the phenomenology, the spatial scale is taken in the longitudinal, say, in x-direction. By definition, we have $\lim_{r\to 0}\frac{\delta u(r)}{r}=\frac{\partial u}{\partial x}$, where the mathematical limit $r\to 0$ physically means $r\to r_{\min}$ in developed turbulence.

[44] If $\alpha=\infty$, that would imply $\|\nabla \boldsymbol{u}\|_{L^\infty}=0$, which contradicts with the regularity of the Navier-Stokes flows. If $\alpha=0$, that would imply $\|\nabla \boldsymbol{u}\|_{L^\infty}=\infty$, which is also absurd. The other possibility, α is indeterminate, is at variance with the assumption 2).

[45] For finite Reynolds number turbulence, deviations from the linear behaviour would be expected at some large, but finite order p because infinitesimally small viscosity is assumed here.

[46] U. Frisch, “Turbulence: The Legacy of A. N. Kolmogorov,” (Cambridge University Press, Cambridge, 1995).

[47] R, Benzi, G. Paladin, S. Patarnello, P. Santangelo and A. Vulpiani, “Intermittency and coherent structures in two-dimensional turbulence,” J. Phys. A: Math. and Gen. **19**, 3771(1986).

[48] B. Lashermes, P. Abry and P. Chainais, “New Insights into the estimation of scaling exponents,” Int. J. of Wavelets, Multiresolution and Information Processing, **2**, 497(2004).

[49] P. Constantin and C. Fefferman, “Scaling exponents in fluid turbulence: some analytic results,” Nonlinearity **7**, 41(1994).

[50] J.D. Gibbon, “A hierarchy of length scales for weak solutions of the three-dimensional Navier-Stokes equations,” to appear in Comm. Math. Sci.

[51] J.D. Gibbon and C.R. Doering, “Intermittency in solutions of the three-dimensional Navier-Stokes equations,” J. Fluid Mech. **478**, 227 (2003).

[52] J.D. Gibbon and C.R Doering, “Intermittency and Regularity Issues in 3D Navier-Stokes Turbulence,” Arch. Rat. Mech. Anal. **177**, 115(2005).

[53] K.R. Sreenivasan, “An update on the energy dissipation rate in isotropic turbulence,” Phys. Fluids, **10**, 528(1998).

[54] K.R. Sreenivasan and P. Kailasnath, “An update on the intermittency exponent in turbulence,” Phys. Fluids A, **5**, 512(1993)

[55] I. Hosokawa and K. Yamamoto, “Intermittency of dissipation in a directly simulated fully-developed turbulence,” Phys. Fluids A, **59**, 401(1989)

[56] D.A. Donzis, K.R. Sreenivasan and P.K. Yeung, “Some results on the Reynolds number scaling of pressure statistics in isotropic turbulence,” J. Phys. Soc. Jpn. **241**, 164(2012)

[57] D.A. Donzis, P.K. Yeung and K.R. Sreenivasan, “Dissipation and enstrophy in isotropic turbulence: Resolution effects and scaling in direct numerical simulations,” Phys. Fluids **20**, 045108(2008).

[58] D.A. Donzis and K.R. Sreenivasan, “Short-term forecasts and scaling of intense events in turbulence,” J. Fluid Mech. **647**, 13(2010).

[59] P.K. Yeung, D.A. Donzis and K.R. Sreenivasan, “Dissipation, enstrophy and pressure statistics in turbulence simulations at high Reynolds numbers,” J. Fluid Mech. to appear (2012).

[60] R.M. Kerr, M. Meneguzzi and T. Gotoh, “An inertial range crossover in structure functions,” Phys. of Fluids **13**, 1985(2001).

[61] S. Almalkie and S.M. de Bruyn Kops, “Energy dissipation rate surrogates in incompressible Navier-Stokes turbulence,” J. Fluid Mech. **697**, 204(2012).

[62] P. Orlandi and G. F. Carnevale, "Nonlinear amplification of vorticity in inviscid interaction of orthogonal lamb dipoles," Phys. Fluids. **19**, 057106(2007).

[63] P. Orlandi and S. Pirozzoli, "Vorticity dynamics in turbulence growth," Theor. Comput. Fluid Dyn. **24**, 247 (2010).